Conformational States of Ras Complexed with the GTP Analogue GppNHp or $GppCH_2p$: Implications for the Interaction with Effector Proteins†

Michael Spoerner,‡ Andrea Nuehs,‡ Petra Ganser,‡ Christian Herrmann,§,|| Alfred Wittinghofer,§ and Hans Robert Kalbitzer*,‡

Institut für Biophysik und physikalische Biochemie, Universität Regensburg, Universitätsstrasse 31, 93053 Regensburg, Germany, and Abteilung Strukturelle Biologie, Max-Planck-Institut für molekulare Physiologie, Otto-Hahn-Strasse 11, 44227 Dortmund, Germany

Received June 9, 2004; Revised Manuscript Received September 17, 2004

ABSTRACT: The guanine nucleotide-binding protein Ras occurs in solution in two different states, state 1 and state 2, when the GTP analogue GppNHp is bound to the active center as detected by ^{31}P NMR spectroscopy. Here we show that Ras(wt)·Mg^{2+}·$GppCH_2p$ also exists in two conformational states in dynamic equilibrium. The activation enthalpy $\Delta H^{\ddagger}_{12}$ and the activation entropy $\Delta S^{\ddagger}_{12}$ for the transition from state 1 to state 2 are 70 kJ mol^{-1} and 102 J mol^{-1} K^{-1}, within the limits of error identical to those determined for the Ras(wt)·Mg^{2+}·GppNHp complex. The same is true for the equilibrium constants K_{12} = [2]/[1] of 2.0 and the corresponding ΔG_{12} of −1.7 kJ mol^{-1} at 278 K. This excludes a suggested specific effect of the NH group of GppNHp on the equilibrium. The assignment of the phosphorus resonance lines of the bound analogues has been done by two-dimensional $^{31}P-^{31}P$ NOESY experiments which lead to a correction of the already reported assignments of bound GppNHp. Mutation of Thr35 in Ras·Mg^{2+}·$GppCH_2p$ to serine leads to a shift of the conformational equilibrium toward state 1. Interaction of the Ras binding domain (RBD) of Raf kinase or RalGDS with Ras(wt) or Ras(T35S) shifts the equilibrium completely to state 2. The ^{31}P NMR experiments suggest that, besides the type of the side chain of residue 35, a main contribution to the conformational equilibrium in Ras complexes with GTP and GTP analogues is the effective acidity of the γ-phosphate group of the bound nucleotide. A reaction scheme for the Ras−effector interaction is presented which includes the existence of two conformations of the effector loop and a weak binding state.

The members of the superfamily of Ras[1]-related guanine nucleotide-binding proteins function as molecular switches using a common principle: they cycle between an inactive GDP-bound and an active GTP-bound state. An estimated 60−100 different proteins belonging to different subfamilies such as Ras, Rho, Rab, and Ran have been identified and shown to regulate a diverse array of signal transduction or transport processes. It is an important question how this switching can be performed effectively and at the same time selectively for a specific subset of proteins interacting with a distinct small GTPase. The answer is to be found in the dynamic behavior of the structural elements involved in the protein−protein interaction.

^{31}P NMR spectroscopy revealed that Ras occurs in two conformational states (states 1 and 2) when it is complexed with the GTP analogue GppNHp (*1*). These two states interconvert with rate constants in the millisecond time scale. The two states are characterized by typical ^{31}P NMR chemical shifts. In state 1 the resonances assigned to the phosphate groups are shifted downfield relative to those of state 2. NMR structural studies have shown that this dynamic equilibrium comprises mainly two regions of the protein called switch I and switch II (*1*−*3*). Solid-state NMR shows that surprisingly even in single crystals of Ras·Mg^{2+}·GppNHp the two conformational states can be observed which are in dynamic equilibrium at ambient temperatures (*4*).

Furthermore, EPR studies of the Mg^{2+} binding site of Ras indicated that the coordination of Thr35 to the γ-phosphate might be transient in solution, suggesting a high flexibility of the side chain and/or the loop containing Thr35 (*5*, *6*). The Gibbs activation energy $\Delta G^{\ddagger}_{12}$ is 59 kJ mol^{-1} at 293 K (*1*). The rate constant of interconversion between the two states can be obtained as 1.1 ms^{-1} at 293 K from a line shape analysis. One of these conformations (state 2) corresponds closely to the conformational state found in the complex with the Ras binding domains (RBD) of Raf kinase (*1*), RalGDS (*7*), AF6 (*8*), and Byr2 (*9*).

A similar behavior is found for the small nuclear GTPase Ran (*10*). In its complex with GTP two different conformational states can be detected by ^{31}P NMR spectroscopy. In state 1 the resonance of the γ-phosphate group is shifted

† This work was supported by the Deutsche Forschungsgemeinschaft, the Fonds der Chemischen Industrie, and the Volkswagenstiftung.

* Corresponding author. Phone: +49 941 943 2594. Fax: +49 941 943 2479. E-mail: hans-robert.kalbitzer@biologie.uni-regensburg.de.

‡ Universität Regensburg.

§ Max-Planck-Institut für molekulare Physiologie.

|| Current address: Institut für Physikalische Chemie I, Universität Bochum, Universitätstrasse 150, 44780 Bochum, Germany.

[1] Abbreviations: DSS, 2,2-dimethyl-2-silapentane-5-sulfonate; DTT, 1,4-dithioerythritol; GppNHp, guanosine 5′-(β,γ-imido)triphosphate; $GppCH_2p$, guanosine 5′-(β,γ-methylene)triphosphate; NMR, nuclear magnetic resonance; RBD, Ras binding domain of the effector molecule; Raf, Raf kinase; RalGDS, guanine nucleotide dissociation stimulator of the small GTPase Ral; Ras, protein product of human H-Ras; wt, wild type.

10.1021/bi0488000 CCC: $30.25
Published on Web 01/25/2005

downfield by 1.74 ppm relative to state 2 whereas the resonances of α- and β-phosphate groups cannot be separated at the magnetic field strength used. In contrast to Ras the equilibrium constant K_{12} is strongly dependent on temperature and varies between 0.67 and 2.33 in the range from 278 and 303 K. The interconversion between the two states in Ran is probably somewhat slower than in Ras; however, the rate constant could not be quantified by NMR spectroscopy. Again, state 2 corresponds to the interaction state with the effector protein, in this case with the nuclear pore protein RanBP1.

A threonine residue located in the effector loop (Thr35 in Ras and Thr42 in Ran) is totally conserved in Ras and Ran and seems to play a pivotal role in the conformational equilibrium. It is involved via its side chain hydroxyl in the coordination of the crucial metal ion and, via its main chain NH, in contacting the γ-phosphate of the nucleotide when complexed to the effector (*11*−*13*) and most probably also in state 2 of uncomplexed Ras and Ran. Replacing this threonine by an alanine or serine residue leads to a complete shift of the equilibrium toward state 1 in solution (*1*, *10*, *14*). These mutants, previously used as partial loss-of-function mutations in cell-based assays, have a reduced affinity to Ras effector proteins without Thr35 being involved in any interaction. The structure of Ras(T35S)·Mg^{2+}·GppNHp was determined by X-ray crystallography (*14*). Whereas the overall structure is very similar to wild type, residues 31−37 and 64−67 from switch I and switch II are completely invisible, indicating that these parts of the structure are either disordered or mobile. ^{31}P NMR data had indicated an equilibrium between two rapidly interconverting conformations, one of which (state 2) corresponds to the structure found in the complex with the effectors. ^{31}P NMR spectra of Ras mutants (T35S and T35A) in the GppNHp form show that the equilibrium is shifted such that they occur predominantly in the nonbinding conformation (state 1). Upon addition of Ras effectors, Ras(T35S) but not Ras(T35A) shifts to positions corresponding to the strong binding conformation.

The structural data were correlated with kinetic experiments that show a two-step binding reaction of wild type and (T35S)Ras with effectors, which requires the existence of a rate-limiting isomerization step for strong binding. This isomerization is not observed with T35A. The results indicate that minor changes in the switch region such as removing the side chain methyl group of Thr35 drastically affect dynamic behavior and in turn interaction with effectors (*14*).

A conformational equilibrium in the interaction site with effectors seems to be a general property of small GTPases. In the present study we will investigate if and how the equilibrium states can be influenced and selected by specific chemical properties of the nucleotide analogue bound to the protein and what is the biological importance of the experimentally found equilibrium. In addition, the assignment of the resonance lines of the bound GppNHp is reinvestigated, which was originally done on the basis of chemical shifts only (*15*).

MATERIALS AND METHODS

Protein Purification. Wild type and mutants of human H-Ras (1−189) or (1−166) were expressed in *Escherichia coli* and purified as described before (*16*). Nucleotide exchange to GppNHp and $GppCH_2p$ was done using alkaline phosphatase treatment in the presence of excess GTP analogue as described by John et al. (*17*). Free nucleotides and phosphates were removed by gel filtration. The final purity of the protein was >95% as judged from sodium dodecyl sulfate−polyacrylamide gel electrophoresis. Ras binding domains of human RalGDS (RalGDS-RBD, amino acids 11−97) and human Raf-1 (Raf-RBD, amino acids 51−131) were expressed in *E. coli* and purified as described before (*18*, *19*).

Sample Preparation. Typically 1 mM Ras·Mg^{2+}·GppNHp or Ras·Mg^{2+}·$GppCH_2p$ was dissolved in 40 mM HEPES/NaOH, pH 7.4, 10 mM $MgCl_2$, 150 mM NaCl, 2 mM DTE, and 0.1 mM DSS in 5% D_2O/95% H_2O. For binding studies highly concentrated (5−7 mM) Raf-RBD or RalGDS-RBD contained in the same buffer was added in appropriate amounts to the samples. When not stated otherwise, full-length Ras(1−189) was used for the studies.

NMR Spectroscopy. ^{31}P NMR spectra were recorded with a Bruker DRX-500 NMR spectrometer operating at 202 MHz. Measurements were performed at various temperatures in a 10 mm probe using 8 mm Shigemi sample tubes. Protons were decoupled during data acquisition by a GARP sequence (*20*) with a strength of the B_1-field of 830 Hz. A Ξ-value of 0.4048073561 reported by Maurer and Kalbitzer (*21*) was used which corresponds to 85% external phosphoric acid contained in a spherical bulb. Temperature was controlled by using the line separation (methylene−hydroxyl) of external ethylene glycol (*22*). Thus, the absolute accuracy of the temperatures given in this study is better than ±0.5 K.

^{31}P longitudinal relaxation times T_1 were measured at 278 K with an inversion recovery sequence using a repetition time of 22 s. The obtained signal integrals were fitted by a three-parameter fit to the equation

$$M_z(t) = M_0 + (M_z(0) - M_0)e^{-t/T_1} \quad (1)$$

with $M_z(t)$ the *z*-magnetization (signal integral) at time *t* and M_0 the magnetization in thermal equilibrium. Protons were decoupled during magnetization recovery by a GARP (*20*) sequence.

^{31}P−^{31}P NOESY (*23*) spectra were recorded with mixing times of 0.2, 0.8, and 2.5 s. Protons were decoupled during t_1 evolution by a proton 180 deg pulse and during t_2 by a GARP (*20*) sequence. The total repetition time was 8.5 s; the total recording time was typically 48−72 h.

Calculation of the Exchange Rates and Thermodynamic Parameters. The exchange rates were calculated by a line shape analysis using the density matrix formalism (*24*) based on a program described by Geyer et al. (*1*) and modified later. The T_2 values given are the relaxation times in absence of chemical exchange. As a first-order correction for the temperature effects on the transversal relaxation time T_2 the dependence of the rotational correlation time τ_{rot} on the viscosity $\eta(T)$ and on the temperature *T* is used. As long as the tumbling is approximately isotropic, τ_{rot} is given by

$$\tau_{rot} = f_s V\eta/kT \quad (2)$$

with f_s a shape factor (equal to 1 for a sphere) and *V* the

effective volume of the molecule. The temperature dependence of the viscosity of the solvent (95% H_2O, 5% D_2O) was calculated with a routine described by Scheiber (*25*) which is implemented in the program AUREMOL (*26*). From these data the viscosity-dependent changes of T_2 were approximated.

Care was taken that the spin systems were completely relaxed in the experiments by using a repetition time of 6 s together with 70 deg pulses. Before the fit of the data the noise level was decreased by multiplying the FID with an exponential filter leading to an additional line broadening of 5 Hz. The difference in the free activation energy $\Delta G^{\ddagger}$, the activation enthalpy $\Delta H^{\ddagger}$, and the activation entropy $\Delta S^{\ddagger}$ were obtained by fitting the temperature dependence of the exchange rates τ_{ex} to the Eyring equation with

$$1/\tau_{ex} = k_1 + k_{-1} \tag{3}$$

For the fit of the data the two-bond phosphorus−phosphorus coupling constants were taken from proton-decoupled spectra of free GppNHp and GppCH$_2$p measured at 278 K in the same buffer used for the experiments with Ras. For GppNHp the coupling constants $^2J_{\alpha\beta}$ of 20.7 ± 0.2 Hz and $^2J_{\beta\gamma}$ of 7.8 ± 0.2 Hz were obtained. For GppCH$_2$p the phosphorus coupling constants $^2J_{\alpha\beta}$ and $^2J_{\beta\gamma}$ are 26.1 ± 0.2 and 8.9 ± 0.1 Hz, respectively. The $^2J_{H\beta}$ and $^2J_{H\gamma}$ constants between the protons of the CH_2 group and the β- and γ-phosphorus are 20.8 ± 0.2 and 19.9 ± 0.2 Hz, respectively. Since protons were decoupled during data acquisition, they could be neglected in the simulation. Small temperature-dependent population shifts expected but not accessible directly experimentally were corrected by assuming that the equilibrium constant $K_{12}(T)$ at temperature T can be approximated by

$$\ln K_{12}(T) = \frac{T_0}{T} \ln K_{12}(T_0) \tag{4}$$

with T_0 set to 278 K.

Calculation of Distances. The NOESY cross-peak volumes V_{ij} and V_{kl} between spin pairs (i,j) and (k,l) are related to their distances r_{ij} and r_{kl} in the initial slope approximation by

$$\frac{r_{ij}}{r_{kl}} = \frac{V_{kl}^{1/6}}{V_{ij}^{1/6}} \tag{5}$$

pH Dependence of Chemical Shifts. The pH dependence of chemical shifts was measured in samples containing 1 mM nucleotide and 0.1 mM DSS in 5% D_2O/95% H_2O. For estimating the optimal magnesium concentration, the $MgCl_2$ concentration was varied in the range from 0 to 40 mM. At 3 mM $MgCl_2$ a plateau in the magnesium-induced chemical shifts was observed for the nucleoside triphosphates at pH 2 and 9. Therefore, this concentration was used for the study of the nucleotide−metal complexes. The pH of the solutions was adjusted by adding HCl or NaOH, respectively, and was determined with a calibrated glass electrode. The dependence of chemical shifts on the pH is usually described by a modified Henderson−Hasselbach equation. In case that more than one pK value is relevant for the dependence of the chemical shift δ on the pH, often a form generalized for N pK values pK_i is given by (see, e.g., ref *27*)

$$\delta = \delta_0 + \sum_{i=1}^{N} (\delta_i - \delta_{i-1}) \frac{10^{pH-pK_i}}{1 + 10^{pH-pK_i}} \tag{6}$$

This equation assumes that all protonation/deprotonation steps occur independently and that the chemical shift changes assigned to each individual protonation/deprotonation step are uncoupled. The more general form (*28*) used here is given by

$$\delta = \frac{\delta_0 + \sum_{i=1}^{N} \delta_i 10^{i pH - \sum_{j=1}^{i} pK_j}}{1 + \sum_{i=1}^{N} \delta_i 10^{i pH - \sum_{j=1}^{i} pK_j}} \tag{7}$$

Note that in eq 7 the pK values are the macroscopic pK_a values of two ionization states of the molecule when one proton is added or removed, whereas in eq 6 the microscopic pK_a of an individual group is concerned.

RESULTS

Chemical Shifts of the Nucleotide Analogues GppNHp and GppCH$_2$p in the Absence and Presence of Magnesium Ions. For an interpretation of the chemical shifts of protein-bound nucleotide analogues, it is necessary to have reliable data of the nucleotides in the absence of proteins. The situation is rather complex since the nucleotide analogues under consideration have at high pH four negatively charged oxygens which can be protonated by decreasing the pH. In addition, the nucleotides are complexed with Mg^{2+} in the protein, which requires the recording of the data also in the presence of this divalent ion. For ATP a wealth of NMR data exists which describes the state of ATP in the presence of Mg^{2+} ions, although the interpretation of the data is rather complicated since in solution a mixture of different states exists, that is, tridentate complexes with Mg^{2+} bound to the three phosphate groups, bidentate complexes with Mg^{2+} bound to the α- and β-phosphate group or the β- and γ-phosphate group, and monodentate complexes with Mg^{2+} bound to one of the negatively charged oxygens of the phosphate group.

Recording the titration data in the absence of the divalent ion is straightforward. However, in the presence of magnesium it is not easy to record data of a well-defined complex since a mixture of different complexes is present in solution (see above). At least, the magnesium concentration was optimized in such a way that the chemical shifts correspond predominantly to the nucleotide in complex with one Mg^{2+} ion. The rate of exchange of nucleoside triphosphates is slow enough for observing the resonances of the metal-free form separately from the metal-complexed form at lower temperatures (*29*). Therefore, the experiments were performed at 278 K to ensure that over the whole pH range a significant contribution of metal-free nucleotide could be detected by additional resonance lines. The ^{31}P resonances were assigned by selective ^{1}H and ^{31}P decoupling experiments.

Figure 1 shows the titration curves for GppCH$_2$p in the absence and presence of Mg^{2+} obtained at 1 mM nucleotide and 3 mM $MgCl_2$ in the pH range from 3 to 13. The most prominent feature is a cross-over of the β- and γ-phosphate

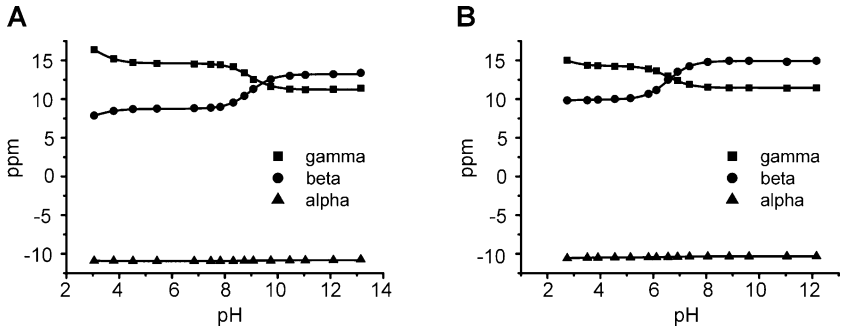

FIGURE 1: Titration curves of free and Mg^{2+}-bound $GppCH_2p$. (A) 2.5 mL of a 1 mM $GppCH_2p$ solution in 95% H_2O and 5% D_2O containing 0.1 mM DSS for indirect referencing. (B) For measurements of the Mg^{2+} complexes 3 mM $MgCl_2$ was added. The pH was varied by adding small amounts of HCl or NaOH to the solutions. The dependence of chemical shifts on the pH values was fitted to eq 7. Measurements were performed in a 10 mm sample tube at 278 K.

Table 1: pH Dependence of Chemical Shifts of Different GTP Analogues[a]

nucleotide	phosphate group	δ_2/ppm	pK_{23}	δ_3/ppm	pK_{34}	δ_4/ppm
$GppCH_2p$	α	(−10.86)	3.2 ± 0.15	−10.93	8.96 ± 0.02	−10.82
	β	(7.14)		8.74		13.22
	γ	(17.85)		14.63		11.23
Mg^{2+}·$GppCH_2p$	α	(−10.83)	2.3 ± 1.5	−10.47	6.57 ± 0.02	−10.33
	β	(9.50)		9.93		14.93
	γ	(16.98)		14.29		11.46
GppNHp	α	(−10.95)	3.4 ± 0.04	−10.80	8.79 ± 0.02	−10.55
	β	(−12.27)		−10.91		−7.76
	γ	(0.20)		−1.64		−0.91
Mg^{2+}·GppNHp	α	(−11.17)	2.0 ± 0.8	−10.34	6.56 ± 0.02	−10.01
	β	(−9.36)		−8.95		−5.46
	γ	(−1.38)		−2.16		−1.02

[a] Data were recorded at 278 K of a solution containing 1 mM nucleotide in the absence or presence of 3 mM $MgCl_2$ in 5% D_2O/95% H_2O. In a first approximation δ_2, δ_3, and δ_4 correspond to the chemical shifts of 2-, 3-, and 4-fold negatively charged nucleotide, and pK_{23} and pK_{34} are the corresponding pK_a values of the three phosphates of the nucleotide. δ_2 values are given in parentheses because the titration up to pH 2.5 only allows an estimation obtained by the fit. For δ_3 and δ_4 the estimated error is ±0.05 ppm.

resonances at ambient pH values; that is, the pattern of resonance lines observed is pH-dependent. Clearly, two pK values are necessary for describing the observed chemical shift changes in the pH range studied. The corresponding pK_a values and chemical shifts are summarized in Table 1. As expected, the apparent pK_a values decrease in the presence of the metal ion. By far the largest effect on the chemical shifts is observed for the *β*-phosphate group whereas also the other two resonances undergo minor shifts. This would suggest a mixture of different metal complexes in solution as observed for ATP (*29*) with a high population of complexes involving the *β*-phosphate of $GppCH_2p$.

The corresponding data were also recorded for GppNHp and analyzed in an analogous manner (Table 1). Again, a strong decrease of pK_a is observable in the presence of $MgCl_2$. At high pH only small chemical shift changes after addition of Mg^{2+} are observed for the resonance of the *γ*-phosphate group, suggesting that the equilibrium is shifted toward complexes which do not involve the *γ*-phosphate group (data not shown).

Conformational States of Ras Complexed with GppCH₂p. Figure 2 shows the ^{31}P NMR spectra of wild-type and (T35S)Ras complexed with the GTP analogue $GppCH_2p$. At low temperature for mutant Ras(T35S) we can observe three phosphorus resonance lines at −12.4, 8.4, and 19.5 ppm whereas for Ras wild type two signals are split into two lines as we have shown previously for Ras if bound to the GTP analogue GppNHp. The resonance lines of the bound nucleotide cannot be assigned simply on the basis of their

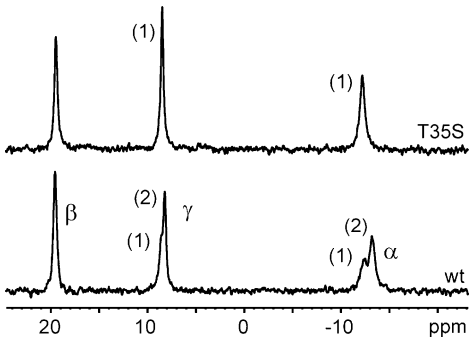

FIGURE 2: Effect of mutation of Thr35 on the ^{31}P NMR spectra of Ras·Mg^{2+}·$GppCH_2p$. The samples contained 1.3 mM Ras(wt)·Mg^{2+}·$GppCH_2p$ (bottom) and 1.4 mM Ras(T35S)·Mg^{2+}·$GppCH_2p$ (top) in 40 mM HEPES/NaOH, pH 7.4, 10 mM $MgCl_2$, 150 mM NaCl, 2 mM DTE, and 0.1 mM DSS in 5% D_2O/95% H_2O, respectively. Data were recorded at 278 K.

chemical shifts since they deviate strongly from those observed in free Mg^{2+}·$GppCH_2p$. In addition, the resonance positions are strongly pH-dependent in the free nucleotide. The ^{31}P chemical shifts of the α-, *β*-, and *γ*-phosphate group in free Mg^{2+}·$GppCH_2p$ are −10.5, 9.9, and 14.3 ppm at pH 5 and −10.3, 14.9, and 11.4 ppm at pH 9 (Table 1), respectively. The assignment of the α-phosphate resonance at −12.8 ppm for bound nucleotide appears to be rather safe; however, the assignments of the two other resonances are not clear. Therefore, we have recorded a proton-decoupled NOESY spectrum of Ras(T35S)·Mg^{2+}·$GppCH_2p$ at 278 K. Ras(T35S) was used because it exists in only one confor-

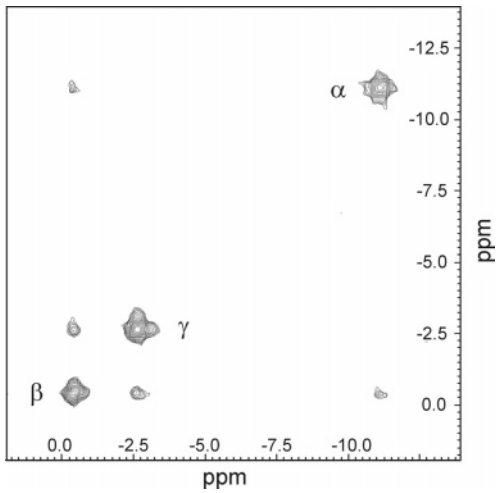

FIGURE 3: Proton-decoupled NOESY spectrum of Ras(T35S)·Mg^{2+}·GppNHp. Data were recorded at 278 K on 0.9 mL of a sample containing 1.8 mM in 40 mM HEPES/NaOH, pH 7.4, 10 mM $MgCl_2$, 2 mM DTE, and 0.1 mM DSS in 5% D_2O/95% H_2O. The mixing time was 2.5 s, the repetition time 8.5 s, and the total acquisition time 78 h. 4096 × 128 time domain data points were sampled.

mational state (see below); therefore, one obtains a better signal-to-noise ratio as well as a better separation of the resonances. It reveals a distance pattern, where the spin with a resonance frequency at −12.8 ppm is close to that at 19.5 ppm and the spin at 19.5 ppm is close to the spins at −12.8 and 8.4 ppm. This allows an assignment of the resonance at 19.5 ppm to the β-phosphate group and the resonance at 8.4 ppm to the γ-phosphate group. In a first estimation the initial slope approximation can be used for the determination of the relative distances r. One obtains a distance ratio $r_{\alpha\beta}/r_{\beta\gamma}$ of 0.99 ± 0.01, which agrees within the limits of error with the values of 0.97−1.07 for the different molecules found in the X-ray-structures of Ras(wt)·Mg^{2+}·GppCH$_2$p (*30*) and the mutant Ras(G12P)·Mg^{2+}·GppCH$_2$p (*31*).

Reassignment of the Resonance Lines of GppNHp Bound to Ras. As can be seen from results of GppCH$_2$p, there are strong differences in the chemical shift values for the phosphates of the free or Ras-bound nucleotides. Therefore, we have examined the resonance assignments of bound GppNHp which were done earlier only on the basis of their chemical shifts (*15*) and accepted in later publications. When the resonance frequencies of free Mg^{2+}·GppNHp (Table 1) at pH 9 (α-phosphate, −10.0 ppm; β-phosphate, −5.5 ppm; γ-phosphate, −1.0 ppm) are compared with the values obtained in the Ras-bound state, the assignments of the α-, β-, and γ-phosphate resonances on the basis of their chemical shifts, for example, for Ras(T35S) at −11.1, −2.6, and −0.3 ppm, seem to be rather unambiguous. A proton-decoupled NOESY spectrum (Figure 3) of Ras(T35S)·Mg^{2+}·GppNHp, recorded at 278 K, reveals a distance pattern, where the spin with a resonance frequency at −0.3 ppm is close to the spins at −11.1 and −2.6 ppm. This allows an assignment of the resonance at −0.3 ppm to the β-phosphate group and the resonance at −2.6 ppm to the γ-phosphate group (Table 2). In first order the initial slope approximation can be used for the determination of the relative distances r. With the above assignments one obtains a distance ratio $r_{\alpha\beta}/r_{\beta\gamma}$ of 1.06 ± 0.01 compared to the value of 1.0 found in the X-ray structure of Ras(wt)·Mg^{2+}·GppNHp (*32*) and 0.98 found for Ras(T35S)·Mg^{2+}·GppNHp (*14*). From the *B*-factors of the X-ray structures an error of 0.4−2 for the distance ratios can be estimated. In conclusion, the assignment reported earlier (*15*) has to be corrected by exchanging the assignment of the β-phosphate group with that of the γ-phosphate group.

Dynamics of the Conformational States of Ras Bound to the Analogues GppCH$_2$p and GppNHp. As observed earlier for the Ras(wt)·Mg^{2+}·GppNHp complex (*1*), at low temperature the resonances of the α- and γ-phosphate group are split into two lines indicating the existence of two conformational states. Raising the temperature leads first to a broadening of these resonances which coalesce then at higher temperatures to single lines. This is the typical behavior expected for two conformational states in a dynamic equilibrium which is slow on the NMR time scale at low temperatures and fast at high temperatures. The chemical shift differences reporting the conformational differences are within 0.89 ppm for the α-phosphate group and 0.39 ppm for the γ-phosphate group, comparable to 0.50 and 0.73 ppm found for GppNHp (Table 2). This suggests that also the conformers reported by the ^{31}P NMR shifts are similar but not identical for the two GTP analogues.

Thr35 is known to be hydrogen-bonded by its backbone amide to the γ-phosphate group of GppNHp and by its hydroxyl group to the magnesium ion in the Ras−effector complexes (*11*−*13*). Replacing this crucial residue by a

Table 2: ^{31}P Chemical Shifts and Conformational States of Ras Complexed with Different GTP Analogues[a]

	α-phosphate		β-phosphate		γ-phosphate		
Ras complex	δ_1/ppm	δ_2/ppm	δ_1/ppm	δ_2/ppm	δ_1/ppm	δ_2/ppm	K_{12}
Ras(wt)·Mg^{2+}·GppCH$_2$p	−12.37	−13.26	19.54		8.59	8.20	2.0
Ras(T35S)·Mg^{2+}·GppCH$_2$p	−12.23		19.47		8.48		<0.05
Ras(wt)·Mg^{2+}·GppNHp[b]	−11.20	−11.70	−0.25		−2.59	−3.32	1.9
c′Ras(wt)·Mg^{2+}·GppNHp[b]	−11.15	−11.71	−0.27		−2.54	−3.36	1.7
Ras(T35S)·Mg^{2+}·GppNHp[b]	−11.13		−0.26		−2.57		<0.1
Ras(T35A)·Mg^{2+}·GppNHp[b]	−11.09		−0.33		−2.49		<0.05
Ras(G12V)·Mg^{2+}·GppNHp	−11.24	−11.55	−0.01		−2.36	−4.08	0.9

[a] Data were recorded at various temperatures; the shifts actually given were taken from spectra recorded at 278 K. The equilibrium constant K_{12} between state 1 and state 2 is calculated from integrals of the γ-resonances defined by $K_{12} = k_{12}/k_{21} = [2]/[1]$. State 1 and state 2 are two conformational states of the Ras−nucleotide complexes with different chemical shifts. In the Ras(wt)·Mg^{2+}·GppNHp complex state 1 is defined as the state where the γ-resonance is shifted downfield relative to state 2. For the complexes with GppCH$_2$p the labeling of the two states visible by chemical shift differences is selected in a similar way. The state with chemical shifts close to those observed in Ras(T35S) is designated as state 1. For the chemical shift values shown the estimated error is ±0.05 ppm; for the K_{12} values it is ±0.1, respectively. [b] Data were recorded at 278 K and pH 7.4. The data from Spoerner et al. (*14*) were reanalyzed and reassigned. The chemical shifts are slightly different from those reported by Geyer et al. (*1*) due to differences in the referencing method. The truncated variant of Ras with amino acids 1−166 is designated as c′Ras.

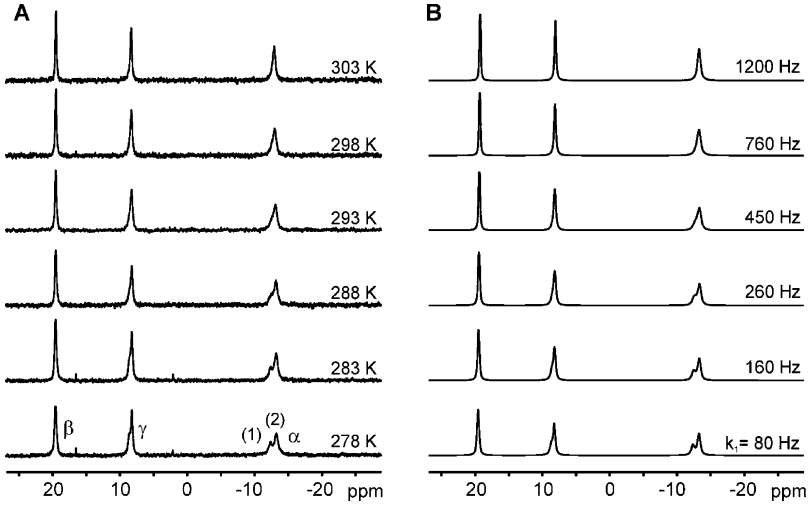

FIGURE 4: Proton-decoupled ^{31}P NMR spectra of Ras(wt)·Mg^{2+}·$GppCH_2p$ at different temperatures. (A) Experimental spectra. (B) Simulated spectra. The sample contained 1.3 mM Ras·Mg^{2+}·$GppCH_2p$ in 40 mM HEPES/NaOH, pH 7.4, 10 mM $MgCl_2$, 2 mM DTE, and 0.1 mM DSS in 5% D_2O/95% H_2O. The absolute temperature was controlled by immersing a capillary with ethylene glycol and measuring the hydroxyl−methylene shift difference (*22*). The experimental data were filtered by an exponential filter leading to an additional line broadening of 5 Hz. The total number of scans per spectrum was 1600−5400. The data were simulated as described in Materials and Methods. The transverse relaxation rates $1/T_2$ at 278 K (in the absence of exchange) obtained from the line shape analysis are 238 s^{-1} for the α-phosphate group of bound $GppCH_2p$ in state 1 and 250 s^{-1} for state 2, 156 s^{-1} for the β-phosphate group in state 1 and state 2, and 263 s^{-1} for state 1 and 192 s^{-1} for state 2 of the γ-phosphate group.

serine residue leads to the disappearance of the ^{31}P NMR lines assigned to state 2 (Figure 2), which is assumed to be the effector binding state of Ras (*1*, *14*). The populations of the different states (state 1 and state 2) in the Ras(wt)·Mg^{2+}·$GppCH_2p$ complex can be obtained from the integration of the resonance lines at low temperature and from the line positions at high temperature. We will show below that the effector binding state 2 is related here again to a high-field shift of the resonances of the α- and γ-phosphate group. The equilibrium constant $K_{12} = [2]/[1]$ calculated from these populations is 2.04 (Table 2) and in a first approximation is independent of the temperature. This is again very similar to the case found in GppNHp.

A line shape analysis of the temperature-dependent data (Figure 4) gives the exchange rate constants. Using the Eyring equation differences in the free activation energy $\Delta G^{\ddagger}$ (Figure 5, Table 4) can be obtained from the rate constants as a function of temperature. The differences in the activation energies correspond to the enthalpies required for breaking a few hydrogen bonds and are within the limits of error almost equal to the GppNHp complex. The errors of $\Delta H^{\ddagger}$ and $\Delta S^{\ddagger}$ are rather large; however, within the limits of error $\Delta H^{\ddagger}$ and $\Delta S^{\ddagger}$ values in the complexes with the two GTP analogues are the same (Table 4). Note that in Table 4 new values for Ras(1−189) for these parameters are given which differ somewhat from the values reported earlier (*1*). They include the new assignment and were recorded under equal conditions like the Ras(wt)·Mg^{2+}·$GppCH_2p$ experiments.

Mutations of Ras in the P-loop, in switch I, and in switch II (*1*) all lead to a shift of the conformational equilibrium toward state 1, however to a different extent. For the complex of GppNHp with the oncogenic mutant Ras(G12V) a line shape analysis was performed (Table 4). At 278 K the Gibbs free energy of activation $\Delta G^{\ddagger}$ is equal within the limits of error to that of the wild-type protein. That is, although for the oncogenic mutant the difference in free energy between state 2 and state 1 ΔG_{12} is 0.24 kJ mol^{-1} and is rather different from −1.48 kJ mol^{-1} found in the wild-type protein,

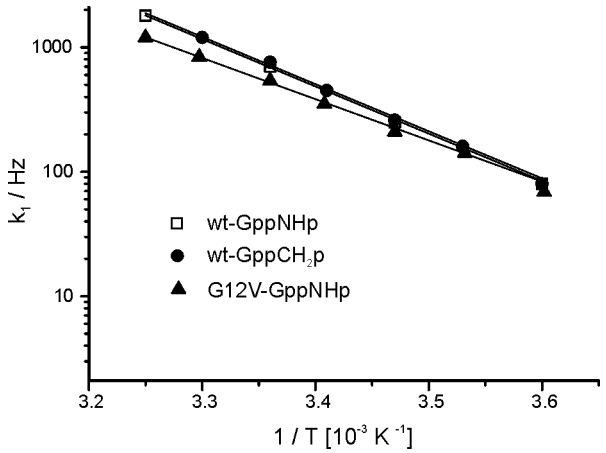

FIGURE 5: Eyring plot of the exchange rates vs the absolute reciprocal temperature for Ras(wt) complexed with Mg^{2+}·GppNHp or Mg^{2+}·$GppCH_2p$ and Ras(G12V)·GppNHp. The rate constants k_{12} were derived from NMR data and fitted to the Eyring equation with the activation enthalpy $\Delta H^{\ddagger}_{12}$ and activation entropy $\Delta S^{\ddagger}_{12}$ as free parameters. The parameters obtained are summarized in Table 4.

the energy necessary to switch between the two states is equal within the limits of error.

Importance of the Two Conformational States for Effector Binding. Addition of effectors to the Ras(wt)·Mg^{2+}·GppNHp complex leads to the disappearance of the ^{31}P NMR lines corresponding to state 1 and appearance of state 2 (*1*, *7*−*9*). Figure 6A shows that this is also observed for Ras(wt) in complex with the GTP analogue $GppCH_2p$: with increasing concentration of the Ras binding domain of Raf kinase the β-phosphate line becomes broader due to the increased molar mass of the complex. The γ-phosphate resonance assigned to state 2 appears to grow with addition of the effector, and the α-phosphate resonance in the complex is shifted to a position between the pair of resonances found for free Ras(wt)·Mg^{2+}·$GppCH_2p$. In Table 3 the chemical shift changes after binding of various Ras binding domains to Ras·Mg^{2+}·

Table 3: ^{31}P Chemical Shifts in Ras Complexed with Different GTP Analogues and Effectors[a]

		α-phosphate			β-phosphate			γ-phosphate		
Ras complex	effector	δ/ppm	Δδ$_1$/ppm	Δδ$_2$/ppm	δ/ppm	Δδ$_1$/ppm	Δδ$_2$/ppm	δ/ppm	Δδ$_1$/ppm	Δδ$_2$/ppm
Ras(wt)·Mg^{2+}·GppCH$_2$p	Raf-RBD	−13.07	−0.70	+0.19	19.60	+0.06		7.90	−0.69	−0.30
Ras(wt)·Mg^{2+}·GppCH$_2$p	RalGDS-RBD	−12.87	−0.50	+0.39	19.69	+0.15		8.06	−0.46	−0.14
Ras(T35S)·Mg^{2+}·GppCH$_2$p	Raf-RBD	−12.97	−0.74	−[e]	19.50	+0.03	−[e]	7.83	−0.65	−[e]
Ras(T35S)·Mg^{2+}·GppCH$_2$p	RalGDS-RBD	−12.87	−0.64	−[e]	19.50	+0.03	−[e]	8.05	−0.43	−[e]
Ras(wt)·Mg^{2+}·GppNHp[b,c]	Raf-RBD	−11.55	−0.35	+0.15	−0.22	+0.03		−3.50	−0.91	−0.18
Ras(wt)·Mg^{2+}·GppNHp[c,d]	RalGDS-RBD	−11.54	−0.34	+0.16	−0.37	−0.12		−3.40	−0.81	−0.08
Ras(T35S)·Mg^{2+}·GppNHp[c]	Raf-RBD	−11.60	−0.47	−[e]	−0.27	−0.01		−3.42	−0.85	−[e]
Ras(T35S)·Mg^{2+}·GppNHp[c]	RalGDS-RBD	−11.54	−0.41	−[e]	−0.29	−0.03		−3.31	−0.74	−[e]
Ras(T35A)·Mg^{2+}·GppNHp[c]	Raf-RBD	−11.10	−0.01	−[e]	−0.31	+0.05	−[e]	−2.49	+0.07	−[e]
Ras(T35A)·Mg^{2+}·GppNHp[c]	RalGDS-RBD	−11.11	−0.02	−[e]	−0.31	+0.05	−[e]	−2.49	+0.07	−[e]
Ras(G12V)·Mg^{2+}·GppNHp	Raf-RBD	−11.60	−0.36	−0.05	−0.23	−0.22		−4.46	+2.05	+0.38

[a] Data were recorded at different temperatures; the shifts δ actually given were taken from spectra recorded at 278 K. The chemical shift changes Δδ upon binding of the effector are defined as $\Delta\delta_1 = \delta - \delta_1$ and $\Delta\delta_2 = \delta - \delta_2$ with δ_1 and δ_2 being the chemical shifts of states 1 and 2 in the free Ras protein. Note that all data were reanalyzed and are expressed in the same reference system. For the chemical shift values shown the estimated error is ±0.05 ppm. [b] Data from Geyer et al. (*1*). [c] Data from Spoerner et al. (*14*). [d] Data from Geyer et al. (*7*). [e] δ_2 of these mutants is not known; therefore, $\Delta\delta_2$ cannot be calculated.

Table 4: Exchange Rates and Thermodynamic Parameters in Different Ras−Nucleotide Complexes[a]

		exchange rate constant (s^{-1})					
protein complex	temp (K)	k_{12}	k_{21}	$\Delta G^{\ddagger}_{12}$ (kJ mol^{-1})	$\Delta H^{\ddagger}_{12}$ (kJ mol^{-1})	$T\Delta S^{\ddagger}_{12}$ (kJ mol^{-1})	ΔG_{12} (kJ mol^{-1})
Ras(wt)·Mg^{2+}·GppCH$_2$p	278	80	39	41 ± 5	63 ± 3	29 ± 2	−1.65 ± 0.15
	288	260	131				
	298	740	391				
Ras(wt)·Mg^{2+}·GppNHp[b]	278	80	42	42 ± 5	70 ± 3	28 ± 2	−1.48 ± 0.15
	288	250	135				
	298	700	387				
Ras(G12V)·Mg^{2+}·GppNHp	278	70	78	41 ± 7	64 ± 4	22 ± 3	0.24 ± 0.25
	288	210	232				
	298	540	596				

[a] The rate constants k_{12} and k_{21} were calculated by a line shape analysis based on the density matrix formalism as described in Materials and Methods. The free activation energies $\Delta G^{\ddagger}_{12}$, the activation enthalpies $\Delta H^{\ddagger}_{12}$, and the activation entropies $\Delta S^{\ddagger}_{12}$ were calculated from the temperature dependence of k_{12} on the basis of the Eyring equation with the errors derived from the fit. The states are defined as in Table 2. ΔG_{12} is the difference in free energy between state 2 and state 1. [b] Note that the values given differ somewhat from those given by Geyer et al. (*1*) since the absolute temperature was controlled independently and the new assignment is considered.

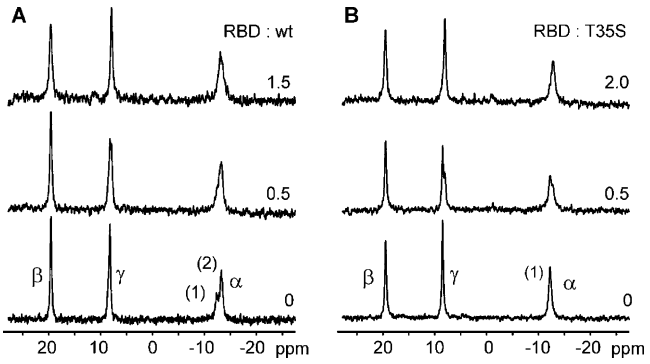

FIGURE 6: Interaction of the Ras binding domain of Raf kinase with Ras(wt)·Mg^{2+}·GppCH$_2$p. Initially, the sample contained 1.3 mM Ras·Mg^{2+}·GppCH$_2$p (A) and 1.3 mM Ras(T35S)·Mg^{2+}·GppCH$_2$p (B) in 40 mM HEPES/NaOH, pH 7.4, 10 mM MgCl$_2$, 150 mM NaCl, 2 mM DTE, and 0.1 mM DSS in 5% D$_2$O/95% H$_2$O, respectively. A solution of 6.8 mM Raf-RBD dissolved in the same buffer was added in increasing amounts. The molar ratios of Raf-RBD/Ras are indicated. All spectra were recorded at 278 K.

GppCH$_2$p and Ras·Mg^{2+}·GppNHp are summarized. For state 2 of Ras(wt)·Mg^{2+}·GppCH$_2$p a similar pattern is found after binding of Raf-RBD or RalGDS-RBD (Table 3), although the chemical shift differences to state 2 of the free protein are larger. For the resonance of the α-phosphate group one finds shifts in the interval 0.19 ppm ≤ Δδ ≤ 0.39 ppm, for the β-phosphate group shifts in the interval 0.06 ppm ≤ Δδ ≤ 0.15 ppm, and for the γ-phosphate group shifts in the interval −0.30 ppm ≤ Δδ ≤ −0.14 ppm.

The observed chemical shift changes indicate that state 2 [defined by the chemical shifts in Ras(wt)·Mg^{2+}·GppCH$_2$p] corresponds to state 2 identified earlier in Ras(wt)·Mg^{2+}·GppNHp. This leads to the conclusion that in the presence of the two nucleotide analogues similar conformational states coexist in solution and are characterized by similar chemical shift changes upon binding. In complex with effector−RBD the mutant Ras(T35S)·Mg^{2+}·GppCH$_2$p seems to exist in a conformational state similar to that found for the wild-type effector complex.

Phosphorus Longitudinal Relaxation Times. Phosphorus relaxation times of nucleotides bound to proteins are only rarely described in the literature. Since the phosphorus atoms are somewhat isolated by their shell of oxygen atoms from other spins, rather long T_1 times are to be expected. The T_1 times of the resonances of the three phosphate groups of GppNHp bound to Ras were measured by an inversion recovery experiment at 278 K. Figure 7 shows the three-parameter fit of the data. Since nonselective pulses were used and $\tau_{ex} \ll T_1$, for Ras(wt) the relaxation times of states 1 and 2 are averaged (Table 5). The values obtained for the different phosphate groups of protein-bound GppNHp differ significantly in the case of Ras(T35A), with the highest

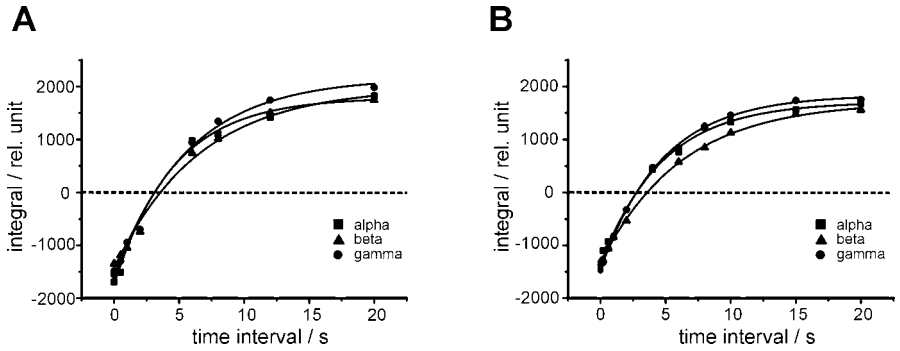

FIGURE 7: T_1 relaxation in Ras(wt)·Mg^{2+}·GppNHp and Ras(T35A)·Mg^{2+}·GppNHp. The integrals of the resonance lines of Ras(wt)·Mg^{2+}·GppNHp (A) and Ras(T35A)·Mg^{2+}·GppNHp (B) are plotted as a function of the time t in an inversion recovery experiment. The lines corresponding to the two conformational states were averaged. Key: α-phosphate (■), β-phosphate (▲), and γ-phosphate (●). The samples contained 1.2 mM Ras·Mg^{2+}·GppNHp in 40 mM HEPES/NaOH, pH 7.4, 10 mM $MgCl_2$, 2 mM DTE, and 0.1 mM DSS in 5% D_2O/95% H_2O. Experiments were performed at 278 K and fitted as described in Materials and Methods. Relaxation times obtained from the fit are listed in Table 5.

Table 5: Phosphorus Relaxation Times in Ras−Nucleotide Complexes

Ras complex	T/K	relaxation times T_1/s of the resonances of α-phosphate	β-phosphate	γ-phosphate
Ras(wt)·Mg^{2+}·GppNHp[a]	278	4.5 ± 0.4	5.3 ± 0.3	5.6 ± 0.4
Ras(T35A)·Mg^{2+}·GppNHp[a]	278	4.7 ± 0.3	6.2 ± 0.3	4.7 ± 0.2

		relaxation times T_2/ms of the resonances of α-phosphate		β-phosphate		γ-phosphate	
Ras complex		1	2	1	2	1	2
Ras(wt)·Mg^{2+}·GppNHp[b]	278	5.8	3.9	4.8	4.8	4.1	7.1
Ras(wt)·Mg^{2+}·$GppCH_2p$[b]	278	4.2	4.0	6.4	6.4	3.8	5.2

[a] Data are from a proton-decoupled, nonselective inversion recovery experiment at 202 MHz phosphorus resonance frequency. [b] The T_2 values were obtained from the line shape analysis. For the values shown the estimated error is ±0.5 ms.

relaxation rate found for the β-phosphate group. For Ras(wt)·GppNHp similar T_1 values for each phosphate were found.

Since the principal values of the chemical shift tensor of Ras·Mg^{2+}·GppNHp were determined earlier by solid-state NMR spectroscopy (*4*), the chemical shift anisotropy $\Delta\sigma$ can be calculated from these values as −180, −157.5, and −137.5 ppm for the α-, β-, and γ-phosphate resonance. Assuming that the rotational reorientation of the bound nucleotide can be described sufficiently well by an isotropic rigid body model, an estimate of the correlation time can be approximated from the viscosity of the solvent and the molecular mass as 15.1 ns at 278 K for Ras(1−189) and 13.6 ns for c′Ras(1−166) (see Materials and Methods). Using these values the contribution of the chemical shift anisotropy on the longitudinal relaxation rate would be 0.32, 0.24, and 0.19 s^{-1} for the α-, β-, and γ-phosphate resonances, respectively. Applying the distances between the phosphate groups from the crystal structure (*32*) with 2.91 Å between the α- and β-phosphate and 2.90 Å between the β- and γ-phosphate of the nucleotide, the calculated contribution of the dipole−dipole interaction is 0.7×10^{-3}, 1.4×10^{-3}, and 0.7×10^{-3} s^{-1}, respectively. The obtained values fit in the limit of error well with the experimental data with $1/T_1$ of 0.22, 0.19, and 0.18 s^{-1} for the α-, β-, and γ-phosphate resonances and indicate that in the Ras−nucleotide system already at 11.7 T (corresponding to a proton resonance frequency of 500 MHz) the main ^{31}P relaxation mechanism is the relaxation via chemical shift anisotropy.

DISCUSSION

Influence of the Nucleotide Bound on the Conformational States of Ras. ^{31}P NMR spectroscopy allows to probe the conformational states of the Ras protein which are coupled to the type of nucleotide present in the active center. In principle, whenever chemical shift changes are visible, they indicate that there is a change of the environment of the observed phosphorus nucleus. For phosphorus resonance spectroscopy on nucleotides it is known that two factors determine mainly chemical shift changes, namely, a conformational strain and electric field effects polarizing the oxygens of the phosphate groups. In addition to these direct effects, long-range effects may occur which can be caused by a structure-dependent change of the anisotropy of the magnetic susceptibility. Here, ring current effects may be the most dominant contribution.

It is obvious that binding to the protein induces large phosphorus chemical shift changes of the phosphate resonances of the nucleotide. This is true not only for the nucleotide binding to Ras but also for other small GTPases such as Ran (*10*) and EF-Tu (*33*). Typically, large chemical shift changes are observed when the nucleotide is bound to the protein. For Ras-bound GTP (*1*) and its analogues $GppCH_2p$ and GppNHp a common shift pattern is observed compared to the free Mg^{2+}−nucleotide complexes in solution: upfield shifts of the α- and γ-phosphate resonances and a strong downfield shift of the β-phosphate resonances compared to the data from the Mg^{2+} complexes of these nucleotides (Tables 1 and 2). Part of the shifts can be

explained by the complexation with magnesium since, in the crystal structures of Ras·Mg^{2+}·GppNHp and Ras·Mg^{2+}·GppCH$_2$p, Mg^{2+} forms a well-defined $\beta-\gamma$ bidentate complex. Since the Mg^{2+} complexes of the free GTP analogues represent a mixture of different complexes in solution, their Mg^{2+}-induced shifts can only be interpreted qualitatively. The maximum downfield shift is found in GppNHp with 2.4 ppm by binding of the metal ion. This value is much smaller than the downfield shifts of 7.5 and 6.4 ppm observed for protein-bound GppNHp and GppCH$_2$p, respectively. The strong downfield shift of the resonance of the β-phosphate group most probably results from a strong polarization of the phosphorus−oxygen bonds. Such a bond polarization in Ras·Mg^{2+}·GppNHp was already discussed by Allin et al. (*34*) as an explanation of strong infrared shifts of the P−O vibrational bands after complexation.

Potential interactions of the phosphate groups can be derived from the X-ray structures published, although one has to be aware that they show differences in details of the effector loop which may reflect the occurrence of different conformational states in solution. Since NMR data indicate that the interaction of Ras with the Ras binding domain of Raf (Raf-RBD) stabilizes the effector loop in a well-defined conformation, the X-ray structure of the Ras-like mutant of Rap1A called Raps [Rap(E30D,K31E)] complexed with Mg^{2+}·GppNHp and Raf-RBD (*11*) can serve as a model. When one looks for groups possibly interacting with the oxygens of the β-phosphate group, the following picture emerges: The *pro-R* nonbridging oxygen of the β-phosphate group is not only bound to the Mg^{2+} ion but may also interact with the amide group and the hydroxyl group of Ser17 and the amide group of Lys16 via a water molecule. The *pro-S* nonbridging oxygen can interact with the amides of Val14, Gly15, and Lys16. The amide of Gly13 most probably interacts with the oxygen positioned between the β- and γ-phosphorus in GTP which is replaced in the structure by the NH group in GppNHp. An especially strong polarization effect is to be expected from the positively charged side chain of Lys16 whose amino group is only 0.29 nm distant from the *pro-S* oxygen of the β-phosphate group.

From the X-ray structure the *pro-S* nonbridging oxygen of the α-phosphate group possibly interacts with the amide groups of Ser17 and Ala18 and the *pro-R* nonbridging oxygen with the amide group of Asp33. One of the nonbridging oxygens of the γ-phosphate is coordinated to the main chain amides of Gly60 and Lys16, and the other nonbridging oxygen is interacting with the main chain amide of Thr35 and the Mg^{2+} ion. In principle, one would expect a deshielding (downfield shift) from these interactions, an especially strong effect for the γ-phosphate which is in contact with the Mg^{2+} ion. Experimentally, an upfield shift is observed. This can be partly explained by the idea that the P−O bonds of these groups are less polarized by the hydrogen bonds to peptide amides than by the hydrogen bonds to the water molecules in solution. In addition, the polarization of the P−O bonds of the β-phosphate group could contribute to the observed chemical shift changes since the whole system of phosphate groups is mutually coupled by the molecular orbitals.

Ring current effects of Tyr32 on the ^{31}P resonance positions may add up to the observed chemical shifts (*1*). This is likely in state 2 and most probably in effector complexes where in the X-ray structure of the Raps−Raf-RBD complex (*11*) the center of the tyrosine ring is closer than 0.52 nm to all phosphorus atoms. The calculated additional shifts should be −0.16, −0.10, and +0.19 ppm for the α-, β-, and γ-phosphate groups, respectively (*1*).

Conformational Equilibria. As reported earlier for the complex of Ras with GppNHp (*1*), Ras exists in more than one conformational state in solution. The populations in the different states change after mutation of Thr35 to alanine or serine (*14*) and are also dependent on the type of nucleotide used (Table 2).

The chemical difference between the nucleotide analogue GppNHp and GTP itself is the replacement of the oxygen bridging the β- and γ-phosphate group by an NH group. Concerning possible interactions with the protein, an oxygen, which potentially can accept a hydrogen bond, is replaced by a group which can potentially donate a hydrogen bond. In addition, it may also influence the polarity and partial charges of the phosphate groups. For the free nucleotides in solution the pK_a of the γ-phosphate group increases from 6.3/4.7 for GTP/Mg^{2+}·GTP to 8.9/6.3 for GppNHp/Mg^{2+}·GppNHp (Table 1) (*35*).

When the NH group in the GTP analogue GppNHp is replaced by a CH_2 group in GppCH$_2$p, the polar group is replaced by an apolar group with completely different properties. Nevertheless, the pK_a values of 9.0 and 6.6 for free nucleotide and Mg^{2+}·nucleotide are quite similar to that of the GppNHp complex.

Surprisingly, although chemically very different, the two analogues bound to Ras are almost indistinguishable in terms of the conformational equilibria. The equilibrium constants K_{12} are identical in the limits of error with values close to 2 (Table 2) and differ significantly from that observed with GTP itself (>10) (*1*). The dynamic parameters for the conformational transition are very similar: within the limits of error Gibb's free energy of activation $\Delta G^{\ddagger}$ and the activation enthalpy and entropy are identical (Table 4).

Two factors may therefore explain the differences observed for GTP and its analogue: (1) a perturbation of an important interaction of oxygen bridging the β- and γ-phosphate groups and (2) an effect due to the changed pK values of the phosphate groups.

One explanation is in line with the X-ray data, which suggest that the bridging $\beta-\gamma$ oxygen interacts with the amide group of Gly13 and/or the side chain amino group of Lys16. There is increasing evidence that GTP-bound Ras occurs in a structural state corresponding to state 2; that is, K_{12} is greater than 10. Thus these interactions could stabilize state 2 in the GTP form and would be abolished in the complexes with the two analogues.

A second explanation would nicely link mutational data with the differences in pK values of the bound nucleotides. An interesting mutation is the mutation of Thr35 to other types of amino acids. In the effector-bound state (*11*, *12*) Thr35 is hydrogen-bonded by its main chain amide to the γ-phosphate moiety and is coordinated by its hydroxyl group to the magnesium ion. If complexed with GppNHp, the replacement of this residue by an alanine or serine in Ras shifts the conformational equilibrium completely to state 1 (*14*). The same is observed when GppCH$_2$p is bound (Figure 2, Table 2); only one state (state 1) can be observed where the resonances of the α- and γ-phosphate groups are

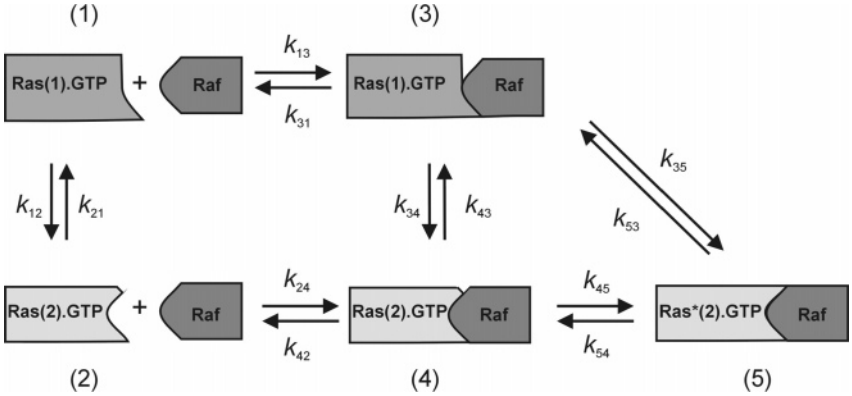

FIGURE 8: Minimum scheme for the Ras−effector interaction with the two conformational states of Ras. It is assumed that the nucleoside triphosphates (GTP or GTP analogues) are always complexed with a Mg^{2+} ion. In the final complex (5) the environment of the nucleotide is probably slightly different from state 2 of Ras [complex (4)], since small chemical shift changes can be observed (Tables 2 and 3).

downfield shifted relative to those representing state 2 with an equilibrium constant $K_{12} < 0.05$. A likely structural model for this population shift would be that in the mutants the side chain of residue 35 is not stabilized by the coordination to the metal ion which leads to a destabilization of the main chain amide hydrogen bond to the γ-phosphate group of the nucleotide. A similar effect may provide a population shift when GTP is replaced by the analogues GppNHp and $GppCH_2p$: the increase of the pK_a value of the γ-phosphate group by more than 2 units implies a significant decrease of the associated free energy of hydrogen bonding for the Thr35 amide group and thus again a destabilization of state 2. As already discussed, the replacement of the amide by a water may contribute to the observed downfield shift. It is clear that this cannot be the only factor influencing the chemical shift difference between the two states since they vary between 0.39 and 0.73 ppm (Table 2). More complex structural rearrangements are to be expected since the whole effector loop is involved in a structural change (*14*). A spectroscopic indication is the observed downfield shift of the α-phosphate resonance in state 1, which suggests again a change of the coordination pattern of the phosphate group, possibly again the replacement of an amide group by a water molecule. A plausible candidate would be the switch I residue Asp33.

The apparent transversal relaxation times of the γ-phosphate groups in the GppNHp complex as well as in the $GppCH_2p$ complex of Ras, obtained from the line shape analysis, are longer in state 2 than in state 1 (Table 5). This may indicate an increased inhomogeneous line broadening by either an increased structural inhomogeneity in state 1 or a real relaxation effect. The same pattern is observed for the longitudinal relaxation when we assume that the value found in the wild-type protein represents an average between the two states but that the value found for Ras(T35A) is representative for state 1. Since the longitudinal relaxation is not directly dependent on inhomogeneous broadening, explanation 1 can be excluded as the main factor. Since we have shown that the chemical anisotropy accounts for almost all relaxation, only a structural change of the ligand sphere of the γ-phosphate group in state 1 with an increased chemical shift anisotropy could explain the data.

Kinetics of the Ras−Effector Interaction. Taking into account the fact that the complexes of Ras with Mg^{2+}·$GppCH_2p$, Mg^{2+}·GppNHp, the fluorescent analogue Mg^{2+}·mGppNHp, and most probably also the other nucleoside triphosphates exist in the two main states Ras(1) and Ras(2) in solution, the binding reaction to Ras binding domain (RBD) thermodynamics requires a minimum scheme as shown in Figure 8. The rate constants k_{12} and k_{21} and the corresponding equilibrium constant K_{12} for the isomerization of the free Ras complexed with the analogues $GppCH_2p$ and GppNHp are known from ^{31}P NMR experiments (Table 2). The NMR chemical shifts of the complexes with the Ras binding domains (RBDs) of the effectors (Table 3) indicate that the final binding state (labeled by an asterisk) is similar but not completely identical to state 2 since significant chemical shift deviations in the bound state from state 2 in the free protein are experimentally observed.

However, kinetic stopped-flow experiments using a fluorescent analogue mGppNHp bound to Ras showed that the binding of effectors to Ras can be described sufficiently well by a two-step model. The data could be fitted satisfactorily by assuming that an initial low-affinity encounter complex isomerizes to the final high-affinity complex (*14*, *36*) and that the Ras−effector complex is highly dynamic, showing both fast association and dissociation kinetics (*14*, *36*, *37*):

$$\text{Ras(1,2)·GTP} + \text{RBD} \underset{k_{31}'}{\overset{k_{13}'}{\rightleftharpoons}} \text{Ras(1,2)·GTP·RBD} \underset{k_{53}'}{\overset{k_{35}'}{\rightleftharpoons}} \text{Ras·GTP·RBD*} \quad (8)$$

It explains the nonlinear dependence of the observed rate constant on the concentration of the RBD which was observed experimentally for Ras·Mg^{2+}·GppNHp (*14*, *36*). The isomerization reaction characterized by k_{35}' becomes rate-limiting with increasing concentrations of Raf-RBD, the rate calculated from this model being 415 s^{-1} at 283 K for wild-type protein, which is not identical to but close to the rate of the interconversion of the two conformations of free Ras·Mg^{2+}·GppNHp measured by NMR under different conditions. If the same reaction is performed with Ras(T35S), the total dissociation constant $K_D = (k_{31}'k_{53}')/(k_{13}'k_{35}')$ increases from 0.05 to 2.1 μM and the isomerization rate constant calculated from this model drops down to 211 s^{-1}. Ras(T35A) behaves differently from the T35S mutant. NMR shows it to be (within the limits of error) completely in the weak-bonding conformational state 1, but in contrast to Ras(T35S) it does not shift into conformation 2 on addition of

Raf-RBD, although the dissociation constant of 7.2 μM to Raf-RBD allows it to bind Raf-RBD under the conditions of this NMR experiment (*14*). This seems to indicate that alanine in position 35, which cannot coordinate to the Mg^{2+} ion as shown for the threonine residue by the 3D structure (*38*, *39*) and expected for serine, forms an effector binding conformation different from the wild type and (T35S)Ras which does not involve a conformational change (*14*).

The simplified scheme (eq 8) would be a special case of the more general equation (Figure 8) if the rate constants k_{13}, k_{31}, k_{35}, and k_{53} would be equal to k_{24}, k_{42}, k_{45}, and k_{54}, respectively. If these constants would be similar, they could be barely distinguished by kinetic methods. The equilibrium can then be described by the condensed equation for most cases. The dissociation constant K_D measured for the equilibrium between free Ras with the concentration c_f = [Ras(1)·Mg^{2+}·GTP] + [Ras(2)·Mg^{2+}·GTP] and the effector protein would be then $K_D = K_{13'}K_{35'}$. However, this is most probably not true (see below) since k_{31} and k_{42} differ most likely by more than 1 order of magnitude.

Since the NMR data indicate that the two states of Ras·GppNHp and Ras·GppCH$_2$p coexisting in solution are structurally different in the effector loop, a region known to be strongly involved in the protein−protein interaction, the simplified picture (eq 8) sufficient for a quantification of the binding reaction is incomplete and does not describe all structural facts known from NMR spectroscopy. With the scheme in Figure 8 and data published or presented here one can give some estimates for the different equilibrium constants in wild-type Ras. K_{12} has been determined experimentally as 2. The T35A mutant shows no isomerization but stays in state 1. This means that the equilibrium constant K_{31} can be approximated by the value of 7 μM given by Spoerner et al. (*14*) for the Ras−Raf interaction and the constant K_{53} must be larger than 10 (since experimentally the final complex of species 5 cannot be observed). In the T35S mutant a main pathway 1−2−4−5 or 1−3−4−5 is likely. The reported value of 68 μM for the encounter complex would lead with a K_{21} of approximately 20 to a K_{42} of about 3.4 μM and a K_{43} of 10. For the total dissociation constant a value of 2.1 μM was reported, which would mean that K_{54} should be 0.03 and K_{53} 0.3 in Ras(T35S). Applying the same values to the wild-type Ras complex but using the experimentally determined equilibrium constant K_{21} of 0.5 between state 1 and state 2 would lead to a value of approximately 0.05 μM for the total dissociation constant of Raf from the wild-type protein, which is close to the experimentally determined value of 0.05 μM (*14*). In summary, a complete consistent set of equilibrium constants for the wild-type Ras·GppNHp interaction with Raf would be $K_{12} = 2.0$, $K_{31} = 7$ μM, $K_{42} = 350$ nM, $K_{35} = 3$, $K_{34} = 0.1$, and $K_{45} = 30$.

Dynamical Processes in Ras and Ras-Related Proteins. It is clear from the NMR data that the switch I region of Ras is in a dynamic equilibrium in the millisecond time scale between (at least) two different conformations. Millisecond mobility has been recently postulated as an important property of domains involved the protein−protein and protein−nucleic acid interaction (*40*). A protein such as Ras has to interact with a number of different proteins such as effectors, GTPase activating proteins, and guanine nucleotide exchange factors. From that it is clear that its interacting surface must be able to adapt to different interaction structures. In addition, it has to be switched fast from the active state with GTP bound to its inactive state with GDP bound and vice versa. These conditions require that the Gibbs free energy difference ΔG between the contributing conformations should not be too large: in the Ras(wt)·Mg^{2+}·GppNHp and the Ras(wt)·Mg^{2+}·GppCH$_2$p complexes ΔG is close to 0 kJ mol^{-1} (Table 4). Since the switching velocity depends on the difference of Gibbs free energy of activation $\Delta G^{\ddagger} = \Delta H^{\ddagger} - T\,\Delta S^{\ddagger}$, these should also be not too large. For wild-type Ras complexed with Mg^{2+}·GppCH$_2$p or Mg^{2+}·GppNHp the activation enthalpies $\Delta H^{\ddagger}_{12}$ are 63 and 69 kJ mol^{-1} and the activation entropies $\Delta S^{\ddagger}_{12}$ are 22 and 28 J mol^{-1} K^{-1}, respectively (Table 4), which correspond to the energy necessary to break a few hydrogen bonds with typical energies of 20 kJ mol^{-1} and are close to the activation enthalpy of 90 kJ mol^{-1} found for the GTP hydrolysis in the absence of GAP (*41*). For the GppNHp complex of the oncogenic mutant Ras(G12V) similar activation parameters are found, indicating that the structural changes involved in the structural transitions involve similar structural intermediates.

Because of the small energetic differences between the two structural states already minor changes in the structure such as replacement of GTP by GppNHp or Thr35 by Ser or Ala can perturb the equilibrium of the structural states significantly (Table 2). They influence only slightly the rate of interconversion of these conformations and decrease the overall affinity to effector proteins. Thr35, being invariant in all Ras-like GTP-binding proteins (and in elongation factors and Gα), is thus apparently conserved not for the structural but rather for the dynamic properties of these switch molecules. Together with Tyr32, it seems to be the amino acid which determines the switching between the GTP and GDP state and the fine tuning in the recognition of different effectors.

Conclusion. Ras exists in (at least) two conformational states which can be identified by NMR spectroscopy. One of the states (state 2) represents the high-affinity binding state for effectors; the other state (state 1) represents a different state (GDP-like?) of the protein with strongly reduced affinity. The equilibrium between the states can be shifted by using different GTP analogues or by specific Ras mutations. The side and main chain interactions of Thr35 with the Mg^{2+}−nucleotide complex play an important role in the conformational equilibrium and are perturbed in state 1. These interactions are also important sensors for the nucleotide state of Ras since they are abolished in the GDP complex of Ras. The transition velocity between the two states and thus the energy of the transition state seem to be largely independent of these factors. State 1 could represent a new target for an anticancer drug development since its stabilization would reduce the strength of the effector interaction considerably.

ACKNOWLEDGMENT

The authors thank Wolfram Gronwald for support in using the program AUREMOL and Burkhard König for helpful discussions.

REFERENCES

1. Geyer, M., Schweins, T., Herrmann, C., Prisner, T., Wittinghofer, A., and Kalbitzer, H. R. (1996) Conformational transitions in p21-

(Ras) and in its complexes with the effector protein Raf-RBD and the GTPase, *Biochemistry 35*, 10308−10320.
2. Kraulis, P. J., Domaille, P. J., Campbell-Burk, S.-L., Van Aken, T., and Laue, E. D. (1994) Solution structure and dynamics of ras p21•GDP determined by heteronuclear three- and four-dimensional NMR spectroscopy, *Biochemistry 33*, 3515−3531.
3. Ito, Y., Yamasaki, K., Iwahara, J., Terada, T., Kamiya, A., Shirouzu, M., Muto, Y., Kawai, G., Yokoyama, S., Laue, E. D., Wälchli, M., Shibata, T., Nishimura, S., and Miyazawa, T. (1997) Regional polysterism in the GTP-bound form of the human c-Ha-Ras protein, *Biochemistry 36*, 9109−9119.
4. Stumber, M., Geyer, M., Graf, R., Kalbitzer, H. R., Scheffzek, K., and Haeberlen, U. (2002) Observation of slow dynamic exchange processes in Ras protein crystals by ^{31}P solid state NMR spectroscopy, *J. Mol. Biol. 323*, 899−907.
5. Bellew, B. F., Halkides, C. J., Gerfen, G. J., Griffin, R. G., and Singel, D. J. (1996) High frequency (139.5 GHz) electron paramagnetic resonance characterization of Mn(II)-H_2(17)O interactions in GDP and GTP forms of p21 ras, *Biochemistry 35*, 12186−12193.
6. Halkides, C. J., Bellew, B. F., Gerfen, G. J., Farrar, C. T., Carter, P. H., Ruo, B., Evans, D. A., Griffin, R. G., and Singel, D. J. (1996) High frequency (139.5 GHz) electron paramagnetic resonance spectroscopy of the GTP form of p21 ras with selective ^{17}O labeling of threonine, *Biochemistry 35*, 12194−12200.
7. Geyer, M., Herrmann, C., Wohlgemuth, S., Wittinghofer, A., and Kalbitzer, H. R. (1997) Structure of the Ras-binding domain of RalGEF and implications for Ras binding and signaling, *Nat. Struct. Biol. 4*, 684−699.
8. Linnemann, T., Geyer, M., Jaitner, T., Block, C., Kalbitzer, H. R., Wittinghofer, A., and Herrmann, C. (1999) Thermodynamic and kinetic characterization of the interaction between the Ras binding domain of AF6 and members of the Ras subfamily, *J. Biol. Chem. 274*, 13556−13562.
9. Gronwald, W., Huber, F., Grünewald, P., Spörner, M., Wohlgemuth, S., Herrmann, C., Wittinghofer, A., and Kalbitzer, H. R. (2001) Solution structure of the Ras binding domain of the protein kinase Byr2 from *Schizosaccharomyces pombe*, *Structure 9*, 1029−1041.
10. Geyer, M., Assheuer, R., Klebe, C., Kuhlmann, J., Becker, J., Wittinghofer, A., and Kalbitzer, H. R. (1999) Conformational states of the nuclear GTP-binding protein Ran and its complexes with the exchange factor RCC1 and the effector protein RanBP1, *Biochemistry 38*, 11250−11260.
11. Nassar, N., Horn, G., Herrmann, C., Block, C., Janknecht, R., and Wittinghofer, A. (1996) The 2.2-angstrom crystal-structure of the Ras-binding domain of the serine threonine kinase c-raf1 in complex with Rap1a and a GTP analogue, *Nat. Struct. Biol. 3*, 723−729.
12. Vetter, I. R., Linnemann, T., Wohlgemuth, S., Geyer, M., Kalbitzer, H. R., Herrmann, C., and Wittinghofer, A. (1999) Structural and biochemical analysis of Ras-effector signaling via RalGDS, *FEBS Lett. 451*, 175−180.
13. Huang, L., Hofer, F., Martin, G. S., and Kim, S.-H. (1998) Structural basis for the interaction of Ras with RalGDS, *Nat. Struct. Biol. 5*, 422−426.
14. Spoerner, M., Herrmann, C., Vetter, I., Kalbitzer, H. R., and Wittinghofer, A. (2001) Dynamic properties of the Ras switch I region and its importance for binding to effectors, *Proc. Natl. Acad. Sci. U.S.A. 98*, 4944−4949.
15. Reinstein, J., Schlichting, I., Frech, M., Goody, R. S., and Wittinghofer, A. (1991) p21 with a phenylalanine 28→leucine mutation reacts normally with the GTPase activating protein GAP but nevertheless has transforming properties, *J. Biol. Chem. 266*, 17700−17706.
16. Tucker, J., Sczakiel, G., Feuerstein, J., John, J., Goody, R. S., and Wittinghofer, A. (1986) Expression of p21 proteins in *Escherichia coli* and stereochemistry of the nucleotide-binding site, *EMBO J. 5*, 1351−1358.
17. John, J., Sohmen, R., Feuerstein, J., Linke, R., Wittinghofer, A., and Goody, R. (1990) Kinetics of interaction of nucleotides with nucleotide-free H-ras p21, *Biochemistry 29*, 6058−6065.
18. Herrmann, C., Martin, G. A., and Wittinghofer, A. (1995) Quantitative analysis of the complex between p21ras and the Ras-binding domain of the human Raf-1 protein kinase, *J. Biol. Chem. 270*, 2901−2905.
19. Herrmann, C., Horn, G., Spaargaren, M., and Wittinghofer, A. (1996) Differential interaction of the Ras family GTP-binding proteins H-Ras, Rap1A, and R-Ras with the putative effector molecules Raf kinase and Ral-guanine nucleotide exchange factor, *J. Biol. Chem. 271*, 6794−6800.
20. Shaka, A. J., Baker, P. B., and Freeman, R. (1985) Computer-optimized decoupling scheme for wideband applications and low-level operation, *J. Magn. Reson. 64*, 547−552.
21. Maurer, T., and Kalbitzer, H. R. (1996) Indirect referencing of ^{31}P and ^{19}F NMR spectra, *J. Magn. Reson. B113*, 177−178.
22. Raiford, D. S., Fisk, C. L., and Becker, E. D. (1979) Calibration of methanol and ethylene glycol nuclear magnetic resonance thermometers, *Anal. Chem. 51*, 2050−2051.
23. Jeener, J., Meier, B. H., Bachmann, P., and Ernst, R. R. (1979) Investigation of exchange processes by two-dimensional NMR spectroscopy, *J. Chem. Phys. 71*, 4546−4553.
24. Rao, B. D. (1989) Nuclear magnetic resonance line-shape analysis and determination of exchange rates, *Methods Enzymol. 176*, 279−311.
25. Scheiber, J. (2003) Diploma Thesis, University of Regensburg.
26. Gronwald, W., and Kalbitzer, H. R. (2004) Automated structure determination of proteins by NMR spectroscopy, *Prog. NMR Spectrosc. 44*, 33−96.
27. Hausser, K. H., and Kalbitzer, H. R. (1991) *NMR in Medicine and Biology. Structure Determination, Tomography, In Vivo Spectroscopy*, Springer, Heidelberg.
28. Freund, J. (1994) Doctoral Thesis, University of Heidelberg.
29. Sontheimer, G. M., Kuhn, W., and Kalbitzer, H. R. (1986) Observation of Mg^{2+}•ATP and uncomplexed ATP in slow exchange by ^{31}P NMR at high magnetic fields, *Biochem. Biophys. Res. Commun. 134*, 1379−1386.
30. Brünger, A. T., Milburn, M. V., Tong, L., de Vos, A. M., Jancarik, J., Yamaizumi, Z., Nishimura, S., Ohtsuka, E., and Kim, S.-H. (1990) Crystal structure of an active form of RAS protein, a complex of a GTP analog and the HRAS p21 catalytic domain, *Proc. Natl. Acad. Sci. U.S.A. 87*, 4849−4853.
31. Schweins, T., Scheffzek, K., Assheuer, R., and Wittinghofer, A. (1997) The role of the metal ion in the p21ras catalysed GTP-hydrolysis: Mn^{2+} versus Mg^{2+}, *J. Mol. Biol. 266*, 847−856.
32. Pai, E., Krengel, U., Petsko, G. A., Goody, R. S., Kabsch, W., and Wittinghofer A. (1990) Refined crystal structure of the triphosphate conformation of H-Ras p21 at 1.35 Å resolution: implications for the mechanism of GTP hydrolysis, *EMBO J. 9*, 2351−2359.
33. Nakano, A., Miyazawa, T., Nakamura, S., and Kaziro, Y. (1980) ^{31}P NMR study of the guanine nucleotide binding of elongation factor Tu from *Thermus thermophilus*, *FEBS Lett. 116*, 72−74.
34. Allin, C., Ahmadian, M. R., Wittinghofer, A., and Gerwert, K. (2001) Monitoring the GAP catalyzed H-Ras GTPase reaction at atomic resolution in real time, *Proc. Natl. Acad. Sci. U.S.A. 98*, 7754−7759.
35. Franken, S. M., Scheidig, A. J., Krengel, U., Rensland, H., Lautwein, A., Geyer, M., Scheffzek, K., Goody, R. S., Kalbitzer, H. R., Pai, E. F., and Wittinghofer, A. (1993) Three-dimensional structures and properties of a transforming and a nontransforming glycine-12 mutant of p21H-ras, *Biochemistry 32*, 8411−8420.
36. Sydor, J. R., Engelhard, M., Wittinghofer, A., Goody, R. S., and Herrmann, C. (1998) Transient kinetic studies on the interaction of Ras and the Ras-binding domain of c-Raf-1 reveal rapid equilibration of the complex, *Biochemisty 37*, 14292−14299.
37. Gorman, C., Skinner, R. H., Skelly, J. V., Neidel, S., and Loewe, P. N. (1996) Equilibrium and kinetic measurements reveal rapidly reversible binding of Ras to Raf, *J. Biol. Chem. 271*, 6713−6719.
38. Pai, E., Kabsch, W., Krengel, U., Holmes, K. C., John, J., and Wittinghofer, A. (1989) Structure of the guanine-nucleotide-binding domain of the Ha-ras oncogene product p21 in the triphosphate conformation, *Nature 341*, 209−214.
39. Milburn, M. V., Tong, L., deVos, A. M., Brünger, A., Yamaizumi, Z., and Nishimura, S. (1990) Molecular switch for signal transduction: structural differences between active and inactive forms of protooncogenic Ras proteins, *Science 247*, 939−945.
40. Feher, V. A., and Cavanagh, J. (1999) Millisecond-timescale motions contribute to the function of the bacterial response regulator protein Spo0F, *Nature 400*, 289−293.
41. Schweins, T., Geyer, M., Kalbitzer, H. R., Wittinghofer, A., and Warshel, A. (1996) Linear free energy relationships in the intrinsic and GTPase activating protein-stimulated guanosine 5′-triphosphate hydrolysis of $p21^{ras}$, *Biochemistry 35*, 14225−14231.

BI0488000